DEVELOPMENT OF METHOD OF AUTOMATICALLY EXTRACTING CRANICAL FEATURE FROM CT IMAGES

PHÁT TRIỂN PHƯƠNG PHÁP TỰ ĐỘNG TRÍCH XUẤT XƯƠNG SỌ TỪ ẢNH CHỤP CẮT LỚP

Nguyen Huu Long[1,*],
Nguyen Thanh Hung[1], Hoang Hong Hai[1]

ABSTRACT

Cranial defect reconstruction, used in Computer Aided Design (CAD) software and 3D printing, helps assess durability, increase surgical accuracy, and reduce surgical costs and risks. This study aims to propose an approach to automatically extract craniofacial fragments using manual methods. The results of craniofacial fragment after automatic extraction are compared with current manual extraction method. Automated extraction reduces treatment time and optimizes 3D part design and fabrication processes.

Keywords: Cranial Defect Reconstruction, 3D Printing, automatically extract, design and fabrication.

TÓM TẮT

Tái tạo khuyết tật sọ, được sử dụng trong phần mềm Computer Aided Design (CAD) và in 3D, giúp đánh giá độ bền, tăng độ chính xác của phẫu thuật, đồng thời giảm chi phí và rủi ro phẫu thuật. Nghiên cứu này nhằm đề xuất phương pháp trích xuất tự động các mảnh sọ mặt bằng phương pháp thủ công. Kết quả mảnh xương sọ sau khi bóc tách tự động so với phương pháp bóc tách thủ công hiện nay. Khai thác tự động giúp giảm thời gian điều trị cho bệnh nhân và tối ưu hóa quy trình thiết kế và chế tạo bộ phận 3D.

Từ khóa: Tái tạo khuyết tật sọ, in 3D, iự động trích xuất, thiết kế và chế tạo.

[1]School of Mechanical Engineering, Hannoi University of Science and Technology
*Email: long.nguyenhuu@hust.edu.vn

1. INTRODUCTION

Skull defects have many causes such as congenital, trauma, brain tumor, which are common problems in surgery [1]. Cranial reconstruction surgery is a big challenge because it is related nerves, brain and eyes [2]. There are many methods to reconstruct the skull, the best method is using autologous bone. However, the use of autologous bone has many limitations due to the insufficient number of donors, the process of bone loss during use. Therefore, there is a need for artificial materials to replace skull surgery. Therefore, it is necessary to have alternative materials in large defects surgery. Specifically, the design of the cranial implant must ensure two factors: the contour of the cranial implant is suitable for the defect of each patient and the material is biocompatible [3]. The bone tissue implanting method uses with alternative materials such as titanium alloys, Polymethyl methacrylate (PMMA), Polyether-ether-ketone (PEEK), [4, 5], etc.,

Currently, the manual extraction method is widely applied due to its simplicity, but it increases the patient's treatment time. Advances in segmentation software have made it increasingly easy to extract the surface of structures of interest automatically or semi-automatically from 3D medical imaging data [6, 7]. The structure of a CT image of the skull often includes bone, layers of muscle tissue, and fat, which affects the extraction process. To minimize the process of extracting the fracture site, we must remove the muscle and fat layer so that the CT image shows only the skeleton component [8].

2. METHODS AND TOOLS

2.1. Methods

In this study, the authors use the method of converting data from Dicom images of patients on CT scanner to pixcel data using OpenCV library [9] and Python language [10].
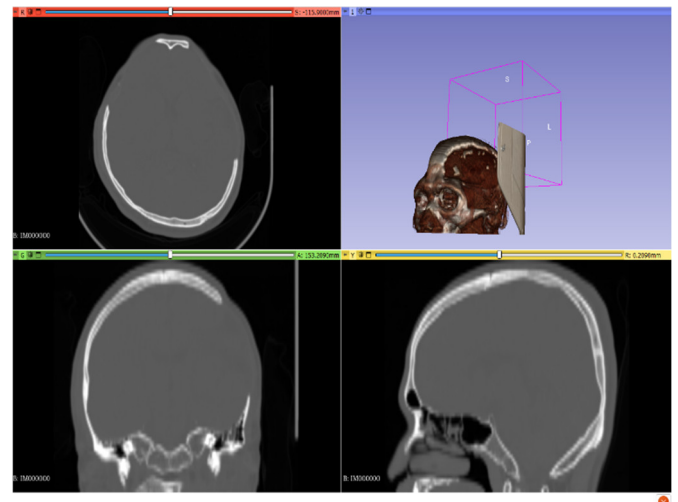

Figure 1. Computed tomography image of the patient's skull before processing

From the patient's CT scan file (DICOMDIR file) through the steps:

• Access to the file DICOMDIR.

• Retrieve data of tomographic images as Dicom files [11].

• Convert to 256-bit image.

• Analyze the acquired image, store the pixel values.

• Update the pixel value of the image after analyzing the dicom file again.

• Merge Dicom files with Slicer 3D.

2.2. Used tools

• Using image processing methods, image filtering, OpenCV library, combining python programming language to analyze and process Dicom images [12].

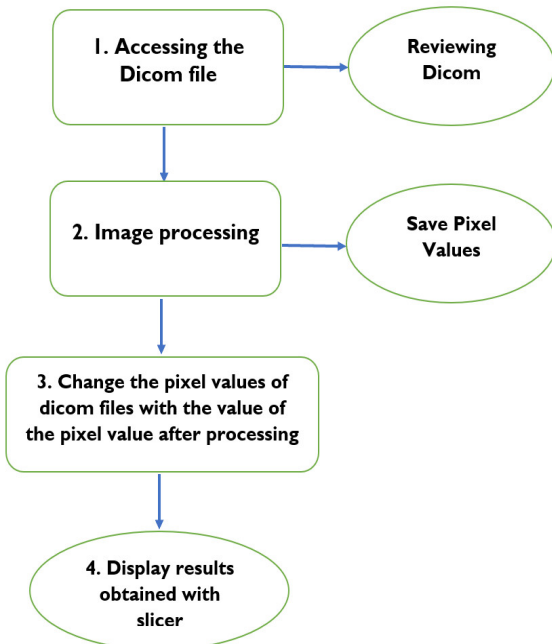• Use Slicer software to display 3D images.

Figure 2. Implementation process

3. EXTRACTION RESULTS AND DISCUSSION

Reading the data in the CT scan file
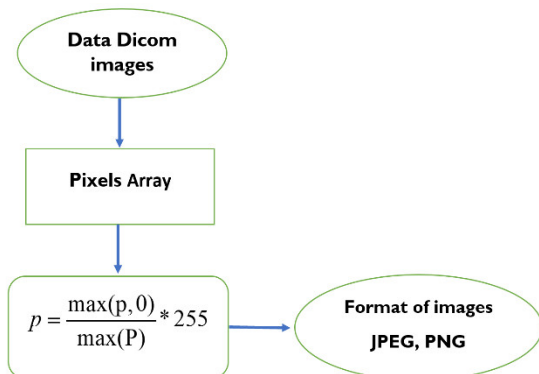
$$p = \frac{\max(p, 0)}{\max(P)} * 255$$

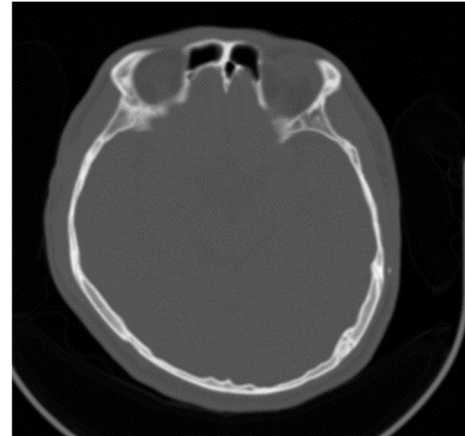Figure 3. Process to convert Dicom images to JPEG and PNG images

Figure 4. Image after converting to JPEG image

Read the data in the CT image file [13], the patient's skull image file is in the form of Dicom, proceed to read the pixel value of the image, obtain the pixel value as a 512x512 2-dimensional array for easy image processing, Convert pixel data from DCM files to common image formats for example .PNG or JPEG.

Convert Dicom images to regular photos show in Figures 3, 4.

Thresholds:

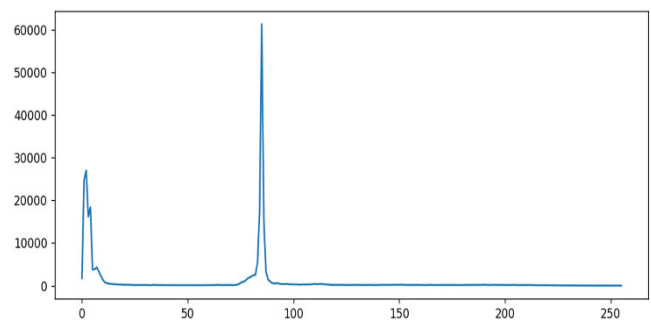For the 255-bit image format, we try to use a basic global threshold.

Figure 5. Histogram of the object

We find that with this tomographic image there are 3 thresholds, however, only the tissue and bone parts are interested, the dark parts are not interested because it is only the background.

When the intensity distributions of objects and background pixels are sufficiently distinct, a single (global) threshold can be used to apply to the entire image. In most applications, there is usually enough variation between images, that even if global thresholding is a suitable approach, an algorithm capable of estimating the threshold value for each is required.

Threshold Algorithm:

• Step 1: Choose an initial estimate for the overall threshold, T.

• Step 2: Segment the image by T in expression (3.1) above. This will create two groups of pixels: G1, consisting

Table 1. Thresholding value

Img	T	deltaT	Img	T	deltaT	Img	T	deltaT
1	134.87	< 0.1	23	134.76	< 0.1	45	134.43	< 0.1
2	134.45	< 0.1	24	134.89	< 0.1	46	134.87	< 0.1
3	134.67	< 0.1	25	134.56	< 0.1	47	134.56	< 0.1
4	134.87	< 0.1	26	134.87	< 0.1	48	134.87	< 0.1
5	134.54	< 0.1	27	134.77	< 0.1	49	134.77	< 0.1
6	134.35	< 0.1	28	134.87	< 0.1	50	134.87	< 0.1
7	134.89	< 0.1	29	134.85	< 0.1	51	134.85	< 0.1
8	134.37	< 0.1	30	134.68	< 0.1	52	134.68	< 0.1
9	134.53	< 0.1	31	134.53	< 0.1	53	134.53	< 0.1
10	134.47	< 0.1	32	134.65	< 0.1	54	134.65	< 0.1
11	134.33	< 0.1	33	134.65	< 0.1	55	134.65	< 0.1
12	134.16	< 0.1	34	134.87	< 0.1	56	134.87	< 0.1
13	134.79	< 0.1	35	134.79	< 0.1	57	134.79	< 0.1
14	134.34	< 0.1	36	134.32	< 0.1	58	134.32	< 0.1
15	134.25	< 0.1	37	134.87	< 0.1	59	134.87	< 0.1
16	134.45	< 0.1	38	134.58	< 0.1	60	134.58	< 0.1
17	134.45	< 0.1	39	134.64	< 0.1	61	134.64	< 0.1
18	134.87	< 0.1	40	134.54	< 0.1	62	134.54	< 0.1
19	134.78	< 0.1	41	134.76	< 0.1	63	134.76	< 0.1
20	134.87	< 0.1	42	134.89	< 0.1	64	134.89	< 0.1
21	134.90	< 0.1	43	134.90	< 0.1	65	134.68	< 0.1
22	134.87	< 0.1	44	134.87	< 0.1	66	134.88	< 0.1
						67	134.66	< 0.1

of pixels with an intensity value > T; and G2, including pixels with the value T.

• Step 3: Calculate the mean (average) intensity values m_1 and m_2 for the pixels in G1 and G2, respectively.

• Step 4: Calculate new threshold value between m_1 and m_2: $T = \frac{1}{2}(m_1+m_2)$ (2)

Repeat steps 2 to 4 until the difference between the values of T in successive iterations is less than the predefined value ΔT.

In results, we have obtained:

T = 134.87704125945

deltaT = 0.056697307767990424

After 20 iterations, the deltaT value is less than 0.1.

Select the threshold value T = 134.

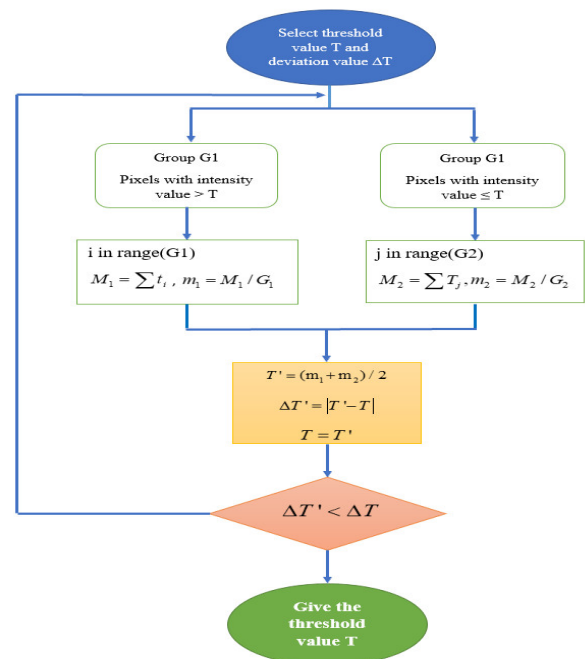Calculate the deviation STDEV: The dispersion of the values compared to the mean is 0.222759.

Figure 6. Investigations of the model accuracy for the Kriging models
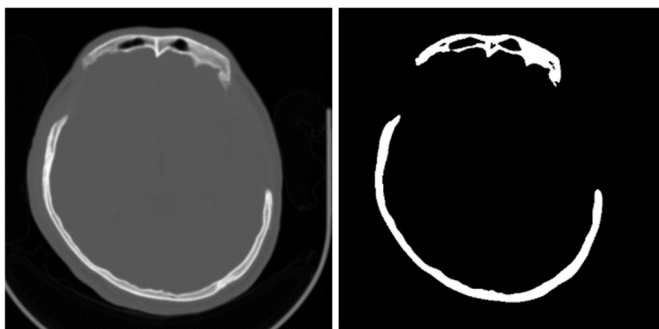
Threshold result:

Figure 7. Threshold results

Noise Filtering:

We use the GaussianBlur filter. The Gaussian filter is one of the most useful filter, implemented by convolutionalizing the input image with a Gaussian filter matrix and then adding them together to form the output image. The general idea is that the value of each pixel depends more on the nearby pixels than on the distant pixels. The weight of the dependency is taken as a Gaussian function (also used in the normal distribution). Assume the image is one-dimensional. The pixel in the center has the greatest weight. Pixels farther from the center has a decreasing weight as their distance from the center increases. Thus, the closer the point is to the center, the more it contributes to the central point value.

To demonstrate to what extent the noise filter process has had on the effort of enhancing proposed method performance. We illustrate the results obtained by applying filtering noise as in figure 8.
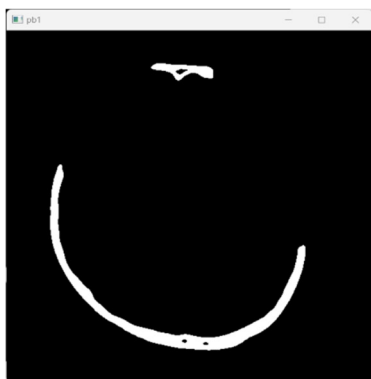

Figure 8. Result in image using thresholding

Converting images to Dicom files:

After that, we convert the processed images back to a DCM file, to display on the 3D Slicer software as figure 9.

Here, we have not investigated the accuracy of 3D skull bone images obtained with automatic extraction compared with manual extraction. To test the accuracy of each extracted image, we compare each extracted image automatically with the manual separation by software. We check every pixel of automatically extracted image and manually extracted image by software. The steps are shown in figure 11.
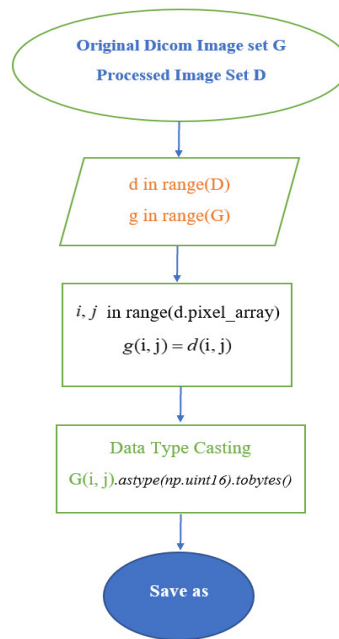

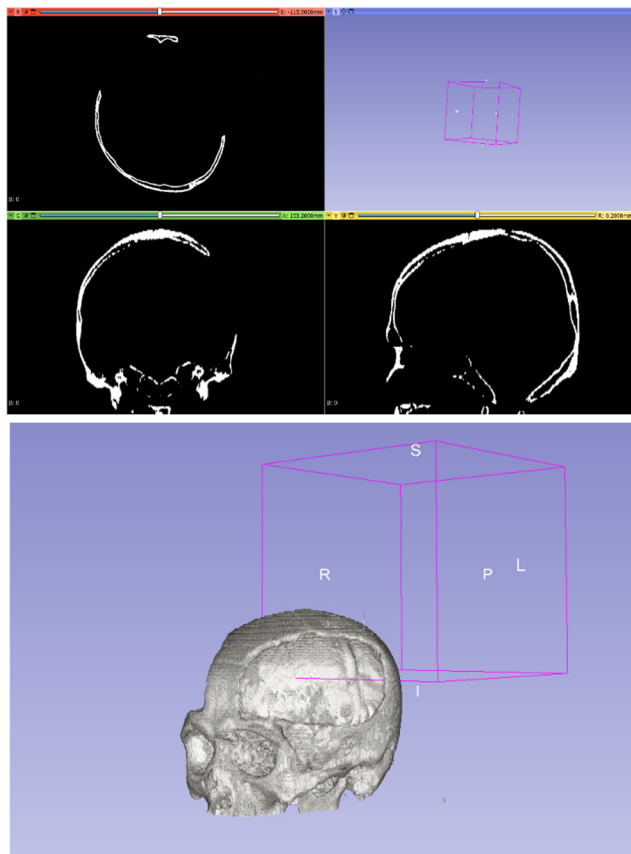Figure 9. Diagram of converting data into Dicom files

Figure 10. Image of patient's skull after separating tissue and brain

From Table 2, we can see that the accuracy of the automatic extraction method is relatively high compared to the manual method. The original images and a lot of redundant information lead to a deviation of about 5%. To the following images more clearly, we see the accuracy less than 2%.
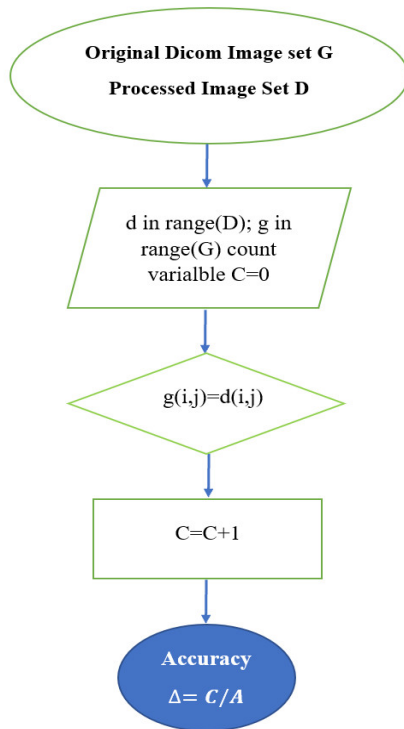
Figure 11. Accuracy evaluation

Table 2. Comparison evaluating between the accuracy of manual and automatic methods on 60 different Dicom image samples

No	Name of Dicom image	Accuracy in comparison to manual
1	IM000010	0.978
2	IM000020	0.994
3	IM000030	0.990
4	IM000040	0.998
5	IM000050	0.993
6	IM000060	0.990

4. CONCLUSION

The proposed method is able to separate the patient's skull, it reduces patient treatment time and optimizes 3D part design and fabrication processes. Although the accuracy of the 3D skull bone image from the automatic extraction method has not been verified in comparision with manual method, but through checking the accuracy of each Dicom image, the accuracy is quite high with an error of less than 5%. It opens the doors to further research development.

REFERENCES

[1]. Goiato M.C., Anchieta R.B., Pita M.S., Dos Santos D.M., 2009. *Reconstruction of skull defects: currently available materials*. J. Craniofac. Surg. 20(5), 1512–1518.

[2]. Moiduddin K., Darwish S., Al-Ahmari A., ElWatidy S., Mohammad A., Ameen W., 2017. *Structural and mechanical characterization of custom design cranial implant created using additive manufacturing*. Electron. J. Biotechnol. 29, 22–31.

[3]. El Halabi F., Rodriguez J.F., Rebolledo L., Hurtós E., Doblaré M., 2011. *Mechanical characterization and numerical simulation of polyether-ether-ketone (PEEK) cranial implants*. J. Mech. Behav. Biomed. Mater. 4(8), 1819–1832.

[4]. Zanotti B., Zingaretti N., Verlicchi A., Robiony M., Alfieri A., Parodi P.C., 2016. *Cranioplasty: review of materials*. J. Craniofac. Surg. 27(8), 2061–2072.

[5]. Khader B.A., Towler M.R., 2016. *Materials and techniques used in cranioplasty fixation: a review*. Mater. Sci. Eng. C 66, 315–322.

[6]. Mohammed M.I., Fitzpatrick A.P., Malyala S.K., Gibson I., 2018. *Customised design and development of patient specific 3D printed whole mandible implant*. In: Solid Freedom Fabrication 2016 Proceedings 27th Annual International Solid Freedom Fabrication Symposium – An Additive Manufacturing Conference SFF 2016, pp. 1708–1717.

[7]. Bücking T.M., Hill E.R., Robertson J.L., Maneas E., Plumb A.A., Nikitichev D.I., 2017. *From medical imaging data to 3D printed anatomical models*. PLoS ONE 12(5), 1–10.

[8]. Torsten B. Moeller, 2016. *Pocket Atlas of Sectional Anatomy*. Caritas Hospital, Germany.

[9]. https://opencv.org/about/.

[10]. https://pydicom.github.io/pydicom/stable/tutorials/filesets.html.

[11]. https://en.wikipedia.org/wiki/DICOM.

[12]. Rafael C. Gonzalez, Richard E. Woods, 2008. *Digital Image Processing*. Pearson Education International.

[13]. Francesco La Rosa, 2017. *A deep learning approach to bone segmentation in CT scans*. Alma Mater Studiorum - Universita di Bologna.

[14]. Sonia Pujol, Steve Pieper, 2014. *Programming in Slicer 4*. Surgical Planning Laboratory, Harvard Medical School.

THÔNG TIN TÁC GIẢ

Nguyễn Hữu Long, Nguyễn Thành Hùng, Hoàng Hồng Hải

Trường Cơ khí, Đại học Bách khoa Hà Nội